THROUGH-TRANSMISSION IMPEDANCE MEASUREMENTS ON MOVING METALLIC SHEETS

Arnold H. Kahn and Michael L. Mester[†]

National Institute of Standards and Technology
Gaithersburg, MD 20899

INTRODUCTION

Eddy current measurement of electrical resistivity provides a method of sensing temperature during metals processing, thus offering a method of feedback control [1,2]. This method assumes a known resistivity-temperature relation for the alloy being processed. However, in many common processing configurations a measurement of the impedance of the coil system can depend on the velocity of the product being tested. In the through-transmission (abbreviated thru-trans) configuration for monitoring moving metallic sheets, the component of the exciting magnetic field normal to the sheet induces an electric field in the sheet transverse to the direction of the velocity. This modifies the induced current distribution and thus changes the shielding of the field at the receiver coil relative to the condition for the static case. This effect is significant even in the case of extruded aluminum moving at 150 ft/min. In high speed rolling, at 1000 ft/min or greater, the effect of velocity is even more significant.

In this report we present the calculation of the effect of a moving conductive sheet on the transfer impedance of a primary and secondary coil in the common thru-trans configuration. We make the assumption that the excitation frequency is sufficiently low that the skin depth is much greater than the sheet thickness, a practical necessity for obtaining a reasonable signal strength in transmission. The thin sheet approximation has been used to advantage by Burke and Rose [3] for modeling cracks. Calculations of the effect of velocity for arbitrary sheet thickness have been presented by Tegopoulos and Kriezis [4] for DC excitation, and by Takehira and Tanaka [5] for an eddy current speedometer. Feng, Deeds, and Dodd [6] report on a flow-rate meter for liquid metals, but for coils in an encircling configuration. In our analysis we produce the impedance plane plots (comma curves) for through-transmission as modified by velocity. Laboratory and plant demonstrations of the effect of velocity will be presented.

[†]Research Associate, The Aluminum Association, Inc.
Now at Babcock and Wilcox, Cleveland OH 44685-0190

Review of Progress in Quantitative Nondestructive Evaluation, Vol. 11
Edited by D.O. Thompson and D.E. Chimenti, Plenum Press, New York, 1992

THEORY

The starting point for analyzing the velocity effect in moving conductive sheets is the vector potential of a single circular current loop. In cylindrical coordinates, the vector potential has only a ϕ component; it is given by

$$A_\phi = \left[\frac{\mu_0 Ia}{2}\right] \int_0^\infty e^{-\alpha|z|}\, J_1(\alpha r) J_1(\alpha a)\, d\alpha, \tag{1}$$

where I is the current, a the radius of the loop, and (r,z) the coordinates of the field point [7]. In Eq.(1), the origin is at the center of the loop, and the ϕ coordinate is ignorable. With a non-vanishing velocity in the x-direction, v_x, it is advantageous to work with the Fourier transforms (FTs) of the in-plane rectangular components of A; these are given by

$$A_{x,\vec{\lambda}} = + \left[\frac{\mu_0 Ia}{2}\right] \frac{1}{2\pi i} \frac{\lambda_y}{\lambda^2} J_1(\lambda a)\, e^{-\lambda|z|} \tag{2a}$$

$$A_{y,\vec{\lambda}} = - \left[\frac{\mu_0 Ia}{2}\right] \frac{1}{2\pi i} \frac{\lambda_x}{\lambda^2} J_1(\lambda a)\, e^{-\lambda|z|} \tag{2b}$$

where $\vec{\lambda}=(\lambda_x,\lambda_y)$ is the two-dimensional FT variable and λ is its length.

For a circular loop which excites eddy currents in a thin sheet of infinite extent, we postulate a solution for the field above and below the sheet in the form:

$$A_x = - \left[\frac{\mu_0 Ia}{2}\right] \frac{1}{2\pi i} \int d\vec{\lambda}\, e^{-i\vec{\lambda}\cdot\vec{r}} \frac{\lambda_y}{\lambda^2} J_1(\lambda a) \left[e^{-\lambda|z-h|} + D_x e^{-\lambda|z|}\right] \tag{3a}$$

$$A_y = + \left[\frac{\mu_0 Ia}{2}\right] \frac{1}{2\pi i} \int d\vec{\lambda}\, e^{-i\vec{\lambda}\cdot\vec{r}} \frac{\lambda_x}{\lambda^2} J_1(\lambda a) \left[e^{-\lambda|z-h|} + D_y e^{-\lambda|z|}\right] \tag{3b}$$

where h is the height of the exciting loop above the conducting sheet, and D_x and D_y are the strengths of the Fourier components of the fields produced by the currents induced in the sheet. (The first terms in the square brackets represent the field in the absence of the sheet.) The values of D_x and D_y, and thus the solution, will be obtained by applying boundary conditions imposed by the conductance of the sheet.

BOUNDARY CONDITIONS

Applying Ampere's circuital relation $\oint H\cdot dl=I$ to paths encircling small regions of the sheet, we obtain the jumps in the tangential components of the H-field at the sheet. In the usual way, we find

$$\Delta H_x = H_x^+ - H_x^- = -J_y\, t \tag{4a}$$

$$\Delta H_y = H_y^+ - H_y^- = J_x\, t, \tag{4b}$$

where the ± signs refer to values just above and below the sheet, and where J is the current density in the sheet of thickness t. This is illustrated in Fig. 1. In the moving sheet the current components are given by

$$J_x = \sigma E_x \tag{5a}$$

$$J_y = \sigma [E_y + (v \times B)_y], \tag{5b}$$

where the additional current due to the velocity appears. Under the assumption of infinitesimal thickness, the conduction of the sheet appears as a boundary condition relating the fields immediately above and below the sheet. Introducing the vector potential, we obtain for the jumps in the field components and the corresponding normal derivatives of the vector potential components:

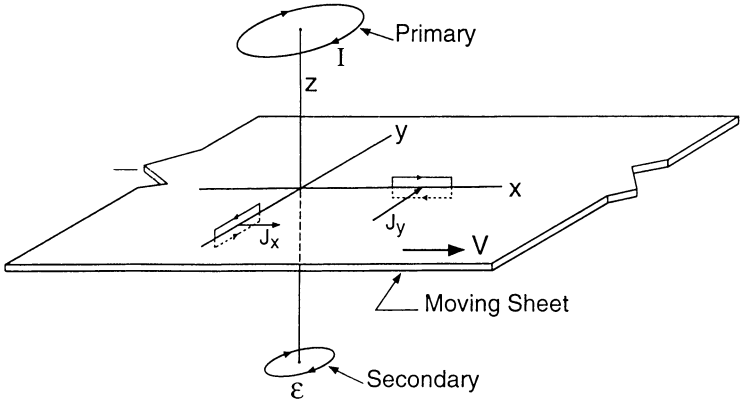

Fig. 1. Diagram of through-transmission geometry. Primary current is I; secondary (receiver) voltage is $\mathcal{E}$. Rectangular paths indicate Ampere circuital integrations encircling currents J_x and J_y.

$$\mu_0 \Delta H_y = \Delta \frac{\partial A_x}{\partial z} = \mu_0 \sigma t \left[-i\omega A_x \right], \tag{6a}$$

$$-\mu_0 \Delta H_x = \Delta \frac{\partial A_y}{\partial z} = \mu_0 \sigma t \left[-i\omega A_y + v_x \left(\frac{\partial A_y}{\partial x} - \frac{\partial A_x}{\partial y} \right) \right]. \tag{6b}$$

In Eqs.(6) the product $\sigma \cdot t$, called the conductance, is held finite while $\sigma \to \infty$ and $t \to 0$. This replacement of the effect of a finite thickness sheet by a boundary condition will be satisfactory if the skin depth is much greater than the thickness of the sheet.

Applying the boundary conditions to the proposed solution, we obtain the coefficients

$$D_x = \frac{\mu_0 \sigma t i \omega e^{-\lambda h}}{2\lambda - i\sigma\mu_0 t\omega} \tag{7a}$$

$$D_y = \frac{\mu_0 \sigma t i e^{-\lambda h}}{2\lambda - i\sigma\mu_0 t(\omega - v_x\lambda_x)} \left[\omega - v_x(\lambda_x+\lambda_y) - \frac{i\lambda_y \omega\sigma\mu_0 t}{2\lambda - i\sigma\mu_0 t\omega} \right] \tag{7b}$$

Detection is accomplished by measuring the emf induced in a receiving coil of radius b placed at location z beneath the sheet. The emf may be found by calculating the time rate of change of the total flux linked by the secondary coil. The final expression for the normalized impedance may be written:

$$Z_N = \frac{-i\int_{-\infty}^{\infty} d\lambda_x \int_{-\infty}^{\infty} d\lambda_y \frac{J_1(\lambda a)\, J_1(\lambda b)}{\lambda^2} e^{-\lambda|z-h|} \left\{ 1 + \frac{1}{\lambda^2} \left[\frac{i\sigma\mu t(\omega - v_x\lambda_x)}{2\lambda - i\sigma\mu t(\omega - v_x\lambda_x)} \lambda_x^2 + \frac{i\sigma\mu t\omega}{2\lambda - i\sigma\mu t\omega} \lambda_y^2 \right] \right\}}{\int_{-\infty}^{\infty} d\lambda_x \int_{-\infty}^{\infty} d\lambda_y \frac{J_1(\lambda a)\, J_1(\lambda b)}{\lambda^2} e^{-\lambda|z-h|}} \tag{8}$$

RESULTS

Fig. 2 shows the calculated impedance curves for the selection of speeds at which measurements were made. Fig. 3 shows the results of thru-trans measurements made on a rotating disk. The calculations were performed for a single turn primary, approximating the experimental coil; the secondary coil was treated as an infinitesimal dipole loop measuring only the on-axis field. Refinement by integrating over a distribution of coil turns, or summation over discrete turns would produce greater accuracy.

The most prominent effect of velocity is the depression of the imaginary part of the normalized impedance in the low frequency limit. At high frequencies the curves coalesce and join the static thru-trans Z-curve.

Experimental verification was accomplished by performing thru-trans measurements on a rotating disk of lithium aluminum alloy of 0.1" thickness. This alloy was chosen because its high room temperature resistivity could be used to simulate the resistivity of more common alloys at elevated temperatures. The coils were 0.5" high, 0.5" in diameter, of 100 turns each, separated 3.5"; they were encased in brass water jackets for cooling.

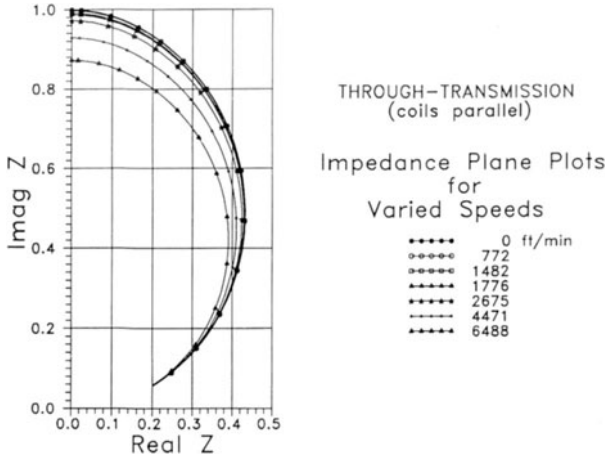

Fig. 2. Imaginary part vs. the real part of the normalized impedance, as calculated from Eq.(8), for speeds used in the experimental measurements.

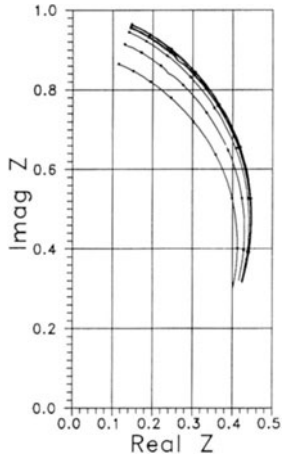

Fig. 3. Plot of measured values of normalized impedance of a lithium-aluminum alloy disk rotated on a lathe. Speeds are tangential velocities at the sensor center with values as in Fig. 2.

The effect of velocity at lower speeds was apparent in an application using the eddy current measurement of resistivity to monitor the temperature of aluminum I-beams during extrusion processing. Fig. 4 shows a typical plot of measured temperature in the I-beams at the exit of the extrusion press as a function of time during the extrusion of three billets. The velocity was 2.7 ft/sec. In the figure, the curves labelled Vanzetti and Williamson refer to the readings of two infrared optical pyrometers; the triangles mark the eddy current conductivity data converted to equivalent temperature and the squares show the readings of a handheld thermocouple. All sensors were initially calibrated together on moving material. The beginning of the figure at time 1400 sec shows the last part of the passage of a billet through the press. At the end of the billet, 1420 sec, an apparent drop of 60°F occurred when the extrusion stopped. This was clearly the effect of cessation of motion. True cooling of the stationary material in the sensor was observed from 1420 sec to 1440 sec. Extrusion of a new billet resumed at 1490 sec. The sharp high spike at 1445 sec was caused by the high resistance weld between the materials of the old and new billets which the programmed analysis interpreted as a hot spot. The drop at 1425 sec was observed repeatedly when the material came to rest at the end of the extrusion of each billet.

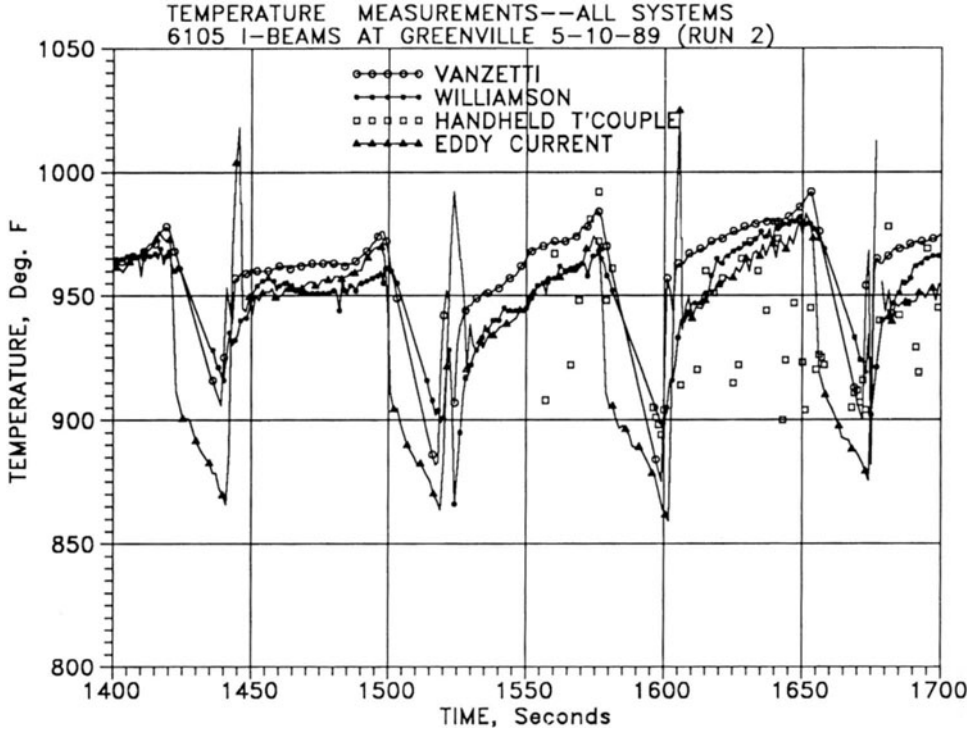

Fig. 4. Measured temperature vs. time of I-beams immediately after being extruded. Triangles indicate eddy current measurement; Vanzetti and Williamson refer to commercial infrared pyrometers. Apparent drop in eddy current reading of approximately 50°F at the end of each extrusion is due to the cessation of motion.

ACKNOWLEDGEMENTS

The authors are grateful to the R.D. Werner Co., Inc. for offering the opportunity to perform on-line testing at its Greenville, PA plant. Help from Dr. Frank Gayle and Mr. Eric Ives at NIST is much appreciated.

REFERENCES

1. M.L. Mester, A.H. Kahn, and H.N.G.Wadley, *Extrusion Technology 1988,* The Aluminum Association, Washington DC, (1988). See p. 259 *et seq.*
2. A.H. Kahn, M.L. Mester, and H.N.G. Wadley, *Intelligent Processing of Materials,* The Materials Society, H.N.G. Wadley and W.E. Eckhart, Jr., eds., pp. 293 *et seq.,* (1990)
3. S.K. Burke and L.R.F. Rose, Proc. R. Soc Lond., A 418, 229 (1988)
4. J.A. Tegopoulos and E.E. Kriezis, *Eddy Currents in Linear Conducting Media,* Elsevier, Amsterdam (1985). See Chap. 10
5. N. Takehira and A. Tanaka, IEE Proceedings, Vol 135, Pt. A, 89 (1988)
6. C.C. Feng, W.E. Deeds, and C.V. Dodd, J. Appl. Phys. 46, 2935 (1975)
7. W.K.H. Panofsky and M. Phillips, *Classical Electricity and Magnetism,* Addison-Wesley, Reading, MA,(1955). See pp. 138-140